Downloaded from rsta.royalsocietypublishing.org

PHILOSOPHICAL TRANSACTIONS OF THE ROYAL SOCIETY A MATHEMATICAL, PHYSICAL & ENGINEERING SCIENCES

Experimental Studies of Earth's Deep Interior: Accuracy and Versatility of Diamond-Anvil Cells

Ho-Kwang Mao and Russell J. Hemley

Phil. Trans. R. Soc. Lond. A 1996 **354**, 1315-1332
doi: 10.1098/rsta.1996.0050

Email alerting service

Receive free email alerts when new articles cite this article - sign up in the box at the top right-hand corner of the article or click **here**

To subscribe to *Phil. Trans. R. Soc. Lond. A* go to:
http://rsta.royalsocietypublishing.org/subscriptions

This journal is © 1996 The Royal Society

Downloaded from rsta.royalsocietypublishing.org

Experimental studies of Earth's deep interior: accuracy and versatility of diamond-anvil cells

By Ho-Kwang Mao and Russell J. Hemley

Geophysical Laboratory and Center for High-Pressure Research, Carnegie Institution of Washington, 5251 Broad Branch Road NW, Washington, DC 20015-1305, USA

Phase equilibria, chemical reactions, equations of state and elasticity investigated at high P–T in candidate materials for the mantle and the core provide an experimental basis for modelling the structure, dynamics and evolution of the Earth's deep interior. During the past three decades, diamond-anvil cells have been developed for experimental simulation of the pressure conditions of the entire Earth in the laboratory. Simultaneous high temperatures have been generated with various heating techniques. Physical and chemical properties of materials have been determined *in situ* at high P–T with microsampling techniques. Further improvements in accuracy and versatility of these measurements are essential for resolving key geophysical problems. Some recent developments in our laboratory are summarized, and assessments of the present status and immediate future of the field are offered.

1. Study of Earth and planetary deep interiors

The theory of plate tectonics has revolutionized our understanding of the motions of the Earth's surface. To understand the dynamics that drives the motions of the plates, however, we must seek answers to such fundamental questions concerning the state of the Earth's mantle and core as: what are the radial and lateral distributions of temperature, pressure, chemical composition, mineralogical constitution and physical properties throughout the Earth? What are the dynamic structures of convection layers and discontinuities, and how are they coupled to each other and to the surface plates chemically and physically? How did the Earth evolve to its present state? What is the nature of the geodynamo which generates the Earth's present magnetic field and is responsible for its previous reversals?

Advances in this area rely on several related disciplines including field observations, theoretical modelling and laboratory measurements. Remote observations with seismic, geomagnetic, gravitational, geodetic and geochemical techniques have obtained detailed information about properties of the Earth's interior. Simulations of convection have been achieved with advanced computer modelling. Advances in high-pressure experimentation with diamond cells, multi-anvil apparatus and dynamic compression have greatly extended the attainable P–T range, and properties of materials over the conditions of the entire Earth can now be measured. We are at the stage of witnessing major breakthroughs in understanding the complete global dynamics in which plate tectonics is the surface manifestation.

Interior models of other planets, including their static and dynamic structures,

Phil. Trans. R. Soc. Lond. A (1996) **354**, 1315–1332
Printed in Great Britain

© 1996 The Royal Society
TEX Paper

The Royal Society is collaborating with JSTOR to digitize, preserve, and extend access to *Philosophical Transactions: Mathematical, Physical and Engineering Sciences.* www.jstor.org

Downloaded from rsta.royalsocietypublishing.org

composition and magnetism, are under similar investigation. For example, it is thought that giant planetary bodies consist of a thick condensed gaseous (H_2 and He) outer shell, an icy (H_2O, NH_3, CH_4, CO and CO_2) inner shell and a small rocky core (Zharkov & Gudkova 1992). Field observations for other planets are, of course, much more scarce and difficult, and theoretical models therefore more speculative, than that of the Earth. Due to the lack of physical and chemical data on gases and ices under the extreme conditions of planetary interiors, interactions among different components within each shell and between shells are practically unknown; the structure and dynamics of planetary interiors are thus poorly defined. Understanding the interiors of planets relies even more heavily on laboratory investigations.

2. Physics and chemistry of Earth and planetary materials

Accurate experimental constraints on Earth and planetary deep interiors require knowledge of a great variety of physical and chemical properties of pertinent materials to be obtained under the corresponding high P–T conditions (figure 1). Important chemical properties include multi-component phase equilibrium, crystal structure, liquid-state and amorphous structure, site occupancy, melting, solution, phase separation, major and minor element partitioning, thermochemical parameters, diffusivity, crystal-field energy and reaction kinetics. Important physical properties include P–T–V equation of state, single-crystal and aggregate elasticity, compressional and shear acoustic velocity, molecular and lattice vibrational frequencies, anelasticity, viscosity, strength, thermal conductivity, electrical conductivity, dielectric parameter, optical parameters, electronic structure and magnetism. Chemical and physical transitions include oxidation–reduction, hydration–dehydration, amorphization–crystallization, order–disorder, high–low electronic spin, insulator–metal and magnetic transitions. Each of these may be profoundly different under high P–T conditions as a result of fundamental alterations of the bonding and interatomic interactions induced by these extreme conditions.

Advances in static and dynamic high-pressure technology have provided new opportunities for direct and accurate experimental measurements in the laboratory. With developments in diamond-cell technology, static high pressures of several hundred GPa can now be reached in the laboratory (Mao *et al.* 1990; Xu *et al.* 1986). Physical and chemical properties of materials can be characterized *in situ* at high pressures. More significantly, the measurement accuracy has been greatly improved. These recent advances should be applied to a broad range of planetary materials, including those studied previously with less accurate techniques. To cover the complete range of properties of planetary materials is an enormous undertaking, even just considering major components alone. For terrestrial planets, the task includes the MgO–FeO–CaO–Al_2O_3–Fe_2O_3–SiO_2–H_2O–CO_2 system for the mantle and the Fe–Ni–Si–K–S–O–H system for the core (at least); for Jovian planets, the planetary gases, fluid, and ices in the H–C–O–N–rare gas system.

3. High-pressure diamond cells

The P–T conditions of the entire Earth and other terrestrial planets, as well as a major portion of the interiors of Jovian planets, are compared with the current and projected accessible ranges of diamond cells in figure 1. Most experiments, including the highest-pressure record, have been performed at the ambient temperature (A in

PHILOSOPHICAL TRANSACTIONS OF THE ROYAL SOCIETY A MATHEMATICAL, PHYSICAL & ENGINEERING SCIENCES

PHILOSOPHICAL TRANSACTIONS OF THE ROYAL SOCIETY A MATHEMATICAL, PHYSICAL & ENGINEERING SCIENCES

Downloaded from rsta.royalsocietypublishing.org

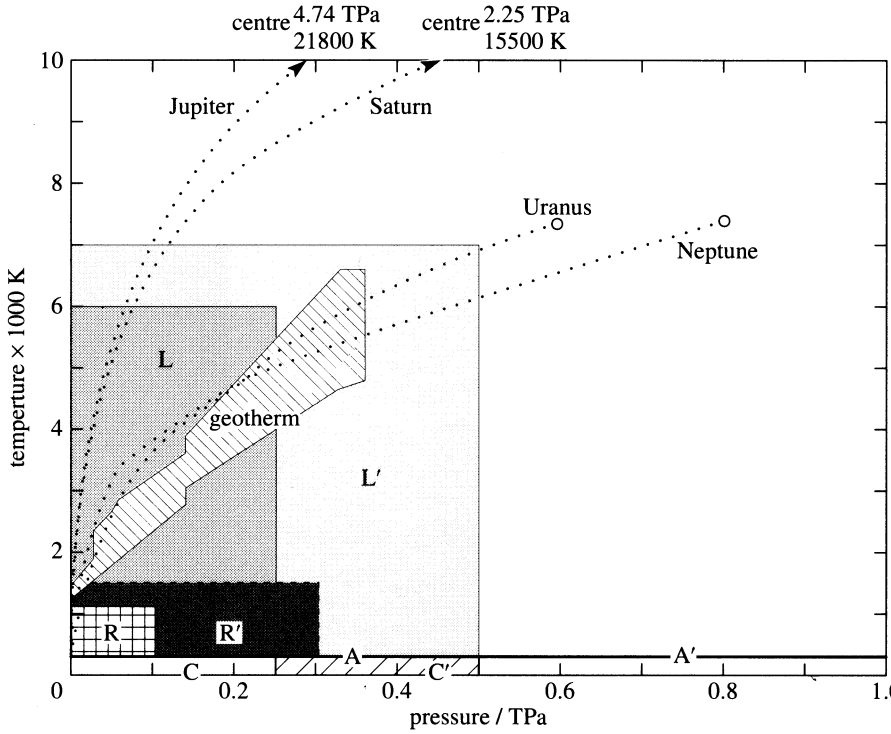

Figure 1. P–T range for diamond-cell experiments. Geotherm: temperature range in terrestrial planetary interiors (Poirier 1991). Dotted curves indicate estimated P–T in Jovian planetary interiors (Zharkov & Gudkova 1992). Presently accessible P–T ranges: A, ambient temperature; C, cryogenic; R, external resistance heating; L, laser heating. Respective ranges for the next stage of development are given by A′, C′, R′ and L′.

figure 1). In such static experiments, pressure conditions are extremely stable. For example, we have held both a quartz and ruby sample at 200 GPa and a hydrogen sample at 10 GPa both for as long as ten years. Cryogenic (C) studies have been particularly useful for fundamental studies of physics and chemistry of the materials. High temperatures at simultaneous high pressures can be applied with external resistance-heating (R) or laser-heating (L) method. The P–T ranges in figure 1 represent the reported maxima rather than the intrinsic limitation of the diamond cell. Expansion of each into a broader range represent feasible goals for the next stage of development.

Diamond windows are transparent to electromagnetic radiation with energies below 5 eV (ultraviolet) and above 5 keV (X-ray). This radiation provides probes for a wide range of properties for samples *in situ* at high pressures. Absorption and reflectance measurements from ultraviolet to far infrared reveal electronic and vibrational information. EXAFS and γ-ray Mössbauer spectroscopies provide information on atoms in specific sites. Fabry–Perot interference measurements contain information on refractive indices, dielectric function, dispersion and sample thickness (Hemley *et al.* 1991). Raman, fluorescence and luminescence spectroscopies are performed in the UV–IR range for a broad range of electronic and structural information. X-ray diffraction is used for structure determination of crystalline (Mao & Hemley 1996) and amorphous materials (Meade *et al.* 1992). Brillouin scattering (Bassett & Brody 1977) and impulsive stimulated scattering (Zaug *et al.* 1992) are used to study elas-

Downloaded from rsta.royalsocietypublishing.org

ticity, anelasticity and thermal diffusivity. Additional techniques which do not use electromagnetic radiation probes include neutron diffraction (Glazkov *et al.* 1988), electrical conductivity, NMR, EPR and DC magnetism (Ishizuka & Amaya 1994). After samples are quenched to ambient conditions, additional probes which are incompatible with the diamond windows, i.e. SEM, TEM, VUV, etc., can be applied. With these techniques, all the aforementioned physical and chemical properties of Earth and planetary materials can be characterized at high P–T.

Trade-offs among maximum P–T range, P–T uniformity, sample size, accessibility, accuracy and sensitivity are essential considerations in these studies. Precise alignment of anvils and the rigidity of the cell body, which are critical factors for reaching ultrahigh pressures, are achieved by mounting diamonds on a precisely fitted long piston and cylinder made of hardened steel (Mao *et al.* 1994). The diamonds are seated on tungsten carbide discs for maximum support. The strong structural configuration often interferes with the optimum conditions for studies of physical properties; for example, there may be limited geometrical access for spectroscopic measurements.

Diamond-cell operation relies on the principle that high pressures are reached by reducing the area over which the force on a sample is applied. Consequently, the sample chamber is extremely small for ultrahigh-pressure experiments. For example, 5 GPa can be reached with a sample chamber of 300 μm diameter × 300 μm thickness (20 nl); whereas for 50 GPa, a typical sample chamber is of order 300 μm diameter × 30 μm (2 nl); and for 300 GPa, it is 20 μm diameter × 3 μm (1 pl). The microscopic samples at the highest pressures are considerably harder to study and generally require the development of new analytical techniques. For most measurements, the maximum P–T is constrained by the detection limit of a specific measurement on the microscopic sample rather than by the P–T capability of the diamond cell.

With the applications of laser and synchrotron light sources (see, for example, Hanfland *et al.* 1992) together with developments in detectors and spectroscopic techniques, advances in the resolution, accuracy and sensitivity for studying microscopic samples at the high P–T have been greatly improved. Unlike the attention-drawing discovery of a new phase, invention of a new technique, or breaking a maximum P–T record, incremental progress in measurement accuracy is usually far less noticeable. However, such a quiet evolution of technique is central for improved understanding of planetary interiors. Cumulative improvements have reached a point that the data obtained with state-of-the-art techniques are qualitatively different from what could be achieved a decade ago. This is illustrated by recent developments in heating, X-ray diffraction and Brillouin scattering techniques at high pressures, as discussed in the following sections. These topics are selected because they provide crucial information for studies of Earth and planetary deep interiors. Emphasis is placed on the discussion of measurement precision and versatility.

4. External resistive heating

Measurements of high-pressure properties at simultaneous high temperatures are essential for modelling static structures and dynamic processes of the Earth. Diamond-cell samples at high pressures can be heated to extremely stable and uniform temperatures (see figure 2) by placing an inner resistance heater (I) close to the diamonds, or by inserting the piston-cylinder assembly (P-C) in an outer furnace (O), or both. The P–T uniformity depends upon the size of sampling area relative to the gradient of P–T. The small sample size in a diamond cell thus has a decisive advan-

PHILOSOPHICAL TRANSACTIONS OF THE ROYAL SOCIETY A MATHEMATICAL, PHYSICAL & ENGINEERING SCIENCES

PHILOSOPHICAL TRANSACTIONS OF THE ROYAL SOCIETY A MATHEMATICAL, PHYSICAL & ENGINEERING SCIENCES

Downloaded from rsta.royalsocietypublishing.org

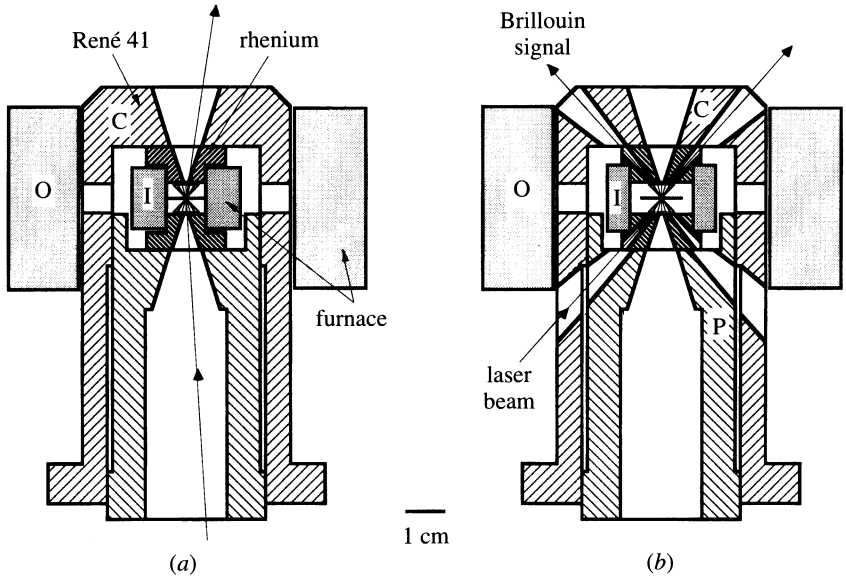

Figure 2. Resistively heated diamond cells: (*a*) for general use and (*b*) for Brillouin scattering measurements.

tage over other more conventional high P–T experimental techniques for petrologic studies. For example, the radial temperature gradient (measured with thermocouples) of a diamond cell with an outer furnace is comparable to that of a cold-seal pressure vessel (Luth & Tuttle 1963), but the dimension of the diamond cell sample is two orders of magnitude smaller, resulting in temperature uniformity within the sample better than ±0.1%. Similarly, a diamond cell with an inner furnace has a temperature gradient comparable to that of a solid-medium piston-cylinder apparatus (Boyd & England 1960), but the sample an order of magnitude smaller, resulting in temperature uniformity of better than ±1%. The pressure can also be truly hydrostatic when fluids (H_2, He, Ne, Ar, N_2, H_2O, CH_4, CO, or CO_2) for the appropriate chemical and physical environments are used as pressure transmitting media (Mao 1989). In principle, the resistively heated diamond cell ultimately provides the best P–T uniformity and sample accessibility for experimentation over a wide pressure range.

Limitations of the maximum temperature are a primary drawback, however. Since the entire diamond cell is heated, the high-temperature environment is detrimental to many parts of the apparatus. Numerous modifications and trade-offs are necessary for different temperature ranges. (*a*) Heating from 300 to 500 K has little effect on the diamond cells, and the quality of measurements is almost as good as that at ambient temperature. The P–T–X phase diagrams of planetary gases and ices are readily studied in this range (Vos *et al.* 1992, 1993). Although the temperature is too low for phase equilibrium studies of silicates or for direct simulation of the geotherm, very accurate measurements in this range can be used to define temperature derivatives of high-pressure properties and to constrain thermal behaviors below Θ_D. (*b*) Most diamond cells are unaffected by heating to the temperature interval of 500–800 K, although temperature may reduce performance of weaker parts. For example, for single-crystal X-ray diffraction, the diamonds are normally supported by beryllium seats which are transparent to the X-ray beam for the maximum accessibility of

Downloaded from rsta.royalsocietypublishing.org

reciprocal space; these may yield in this temperature range. Pressure calibration based on ruby fluorescence becomes unusable due to the temperature broadening of the fluorescence line. Instead, Sm:YAG fluorescence (Hess & Schiferl, 1992) or P–V–T equations of state of gold (Ming *et al.* 1983) and NaCl (Decker 1971) are commonly used for pressure calibration under these conditions. (*c*) Numerous problems emerge between 800 and 1200 K, but can be remedied. Inert gas pressure media become difficult to contain, but are replaced by solid media (e.g. NaCl) which are sufficiently hydrostatic at these temperatures. The hardened steel used for constructing the cell body loses its strength and is replaced by high-temperature metals, such as inconel, René 41, or rhenium. The use of an inert or reducing atmosphere (e.g. argon with 1% hydrogen) protects the diamonds and the rhenium gasket from oxidation. (*d*) Above 1200 K, problems increase while the maximum pressure is greatly reduced. The ultimate limit is approximately 1600 K, above which all high-temperature metals and the diamond become too soft to sustain high pressures.

A design optimized for the entire temperature range is shown in figure 2. Excellent alignment is achieved and maintained by the long piston-cylinder configuration. In order to minimize jamming and binding in the presence of a large temperature gradient, the long contacting surface of the piston-cylinder is reduced to two short bearing sections (with slightly different diameters) at the ends of the long piston and cylinder. The parts (gasket and diamond seats) subjected to the maximum temperature of the inner heater are made of rhenium while the piston-cylinder consists of René 41 and remains below 1200 K. The axial apertures are reduced to 30° cones to provide space for a longer cylindrical inner heater while still providing sufficient accessibility for X-ray diffraction and most absorption, reflection and scattering measurements (figure 2*a*). Brillouin spectroscopy, which benefits from 90° scattering angle, can be obtained with the modification shown in figure 2*b*.

Unprecedented accuracy over a broad range of measurements can be achieved with the uniform and stable P–T conditions of the resistively heated diamond cell. Measurements over this moderate temperature but wide pressure range (figure 1) provide stringent tests of condensed-matter theories to be extrapolated to higher P–T conditions (Fei *et al.* 1992; Mao *et al.* 1991; Stixrude *et al.* 1992). They also directly cover hydrothermal conditions (Bassett *et al.* 1993), the lower temperature portion of the geotherm and the subducting slabs. The phase transition of silicate spinel to lower mantle phases was first achieved with resistively heated diamond cell (Mao & Bell 1971). Recently the phase diagram of FeO, which is possibly the only common major component of both the Earth's metallic core and the oxide mantle, has been mapped out over 100 GPa and 1100 K (Fei & Mao 1994). The results demonstrate that at high P and low T wüstite undergoes a displacive transition from B1 to a rhombohedral structure, and at higher P–T, a second transition to B8 (NiAs) structure (figure 3). Likewise, the phase diagram of FeS has been determined (figure 4). The discovery of a NiAs-structured phase of FeS (IV) has important implications for understanding the Martian core (Fei *et al.* 1995).

5. Laser heating

Laser heating of diamond-cell samples (Bassett & Ming 1972) provides the means of creating static conditions of the Earth's deepest interior (L and L′ in figure 1). Discoveries of lower mantle phases (Liu & Bassett 1986) and studies of melting and subsolidus phase diagrams at lower mantle and core conditions were mostly

PHILOSOPHICAL TRANSACTIONS OF THE ROYAL SOCIETY A MATHEMATICAL, PHYSICAL & ENGINEERING SCIENCES
PHILOSOPHICAL TRANSACTIONS OF THE ROYAL SOCIETY A MATHEMATICAL, PHYSICAL & ENGINEERING SCIENCES

Downloaded from rsta.royalsocietypublishing.org

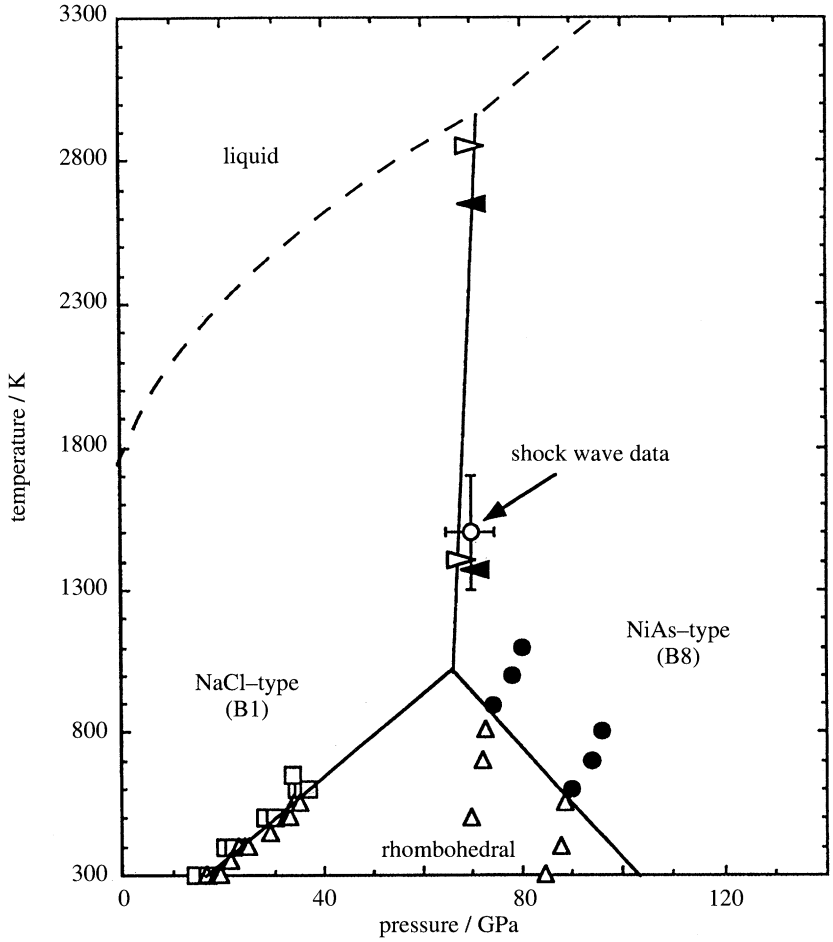

Figure 3. *P–T* phase diagram of FeO (Fei & Mao 1994). Data below 1100 K are from resistance-heated diamond-cell experiments. Three phases of FeO are identified by X-ray diffraction: B1 (square), rhombohedral (triangle) and B8 (solid circle). Data above 1100 K are observations of discontinuities in density or electrical resistivity in shock-wave experiments (open circle, Jeanloz & Ahrens 1980) and laser-heated diamond cells (arrow, Knittle & Jeanloz 1991). The dashed melting curve is from a laser-heated diamond-cell study (Boehler 1992).

achieved with laser-heated diamond cells (see articles by Boehler, Jeanloz & Kavner, and Jephcoat & Besedin in this volume and reviews in Manghnani & Syono (1987) and Syono & Manghnani (1992)). Despite the small size of diamond-cell samples, early work on quenched samples revealed important new insights, as demonstrated for the MgO–FeO–SiO_2 system (Mao *et al.* 1979; Yagi *et al.* 1979). Not only were phases correctly identified in these studies, but the proposed phase diagrams were largely confirmed in much later studies carried out with large-volume presses (Ito & Takahashi 1989). Laser heating has also been used for *in situ* determination of phase transitions (e.g. in iron by Saxena *et al.* 1995; Yoo *et al.* 1995). Figure 3 shows the phase diagram of FeO determined by a combination of laser- (Boehler 1992; Knittle & Jeanloz 1991) and resistance heating (Fei & Mao 1994) techniques.

However, laser heating has its drawbacks. While the samples absorbing the laser beam are heated to thousands of degrees, other parts of the high-pressure apparatus

Downloaded from rsta.royalsocietypublishing.org

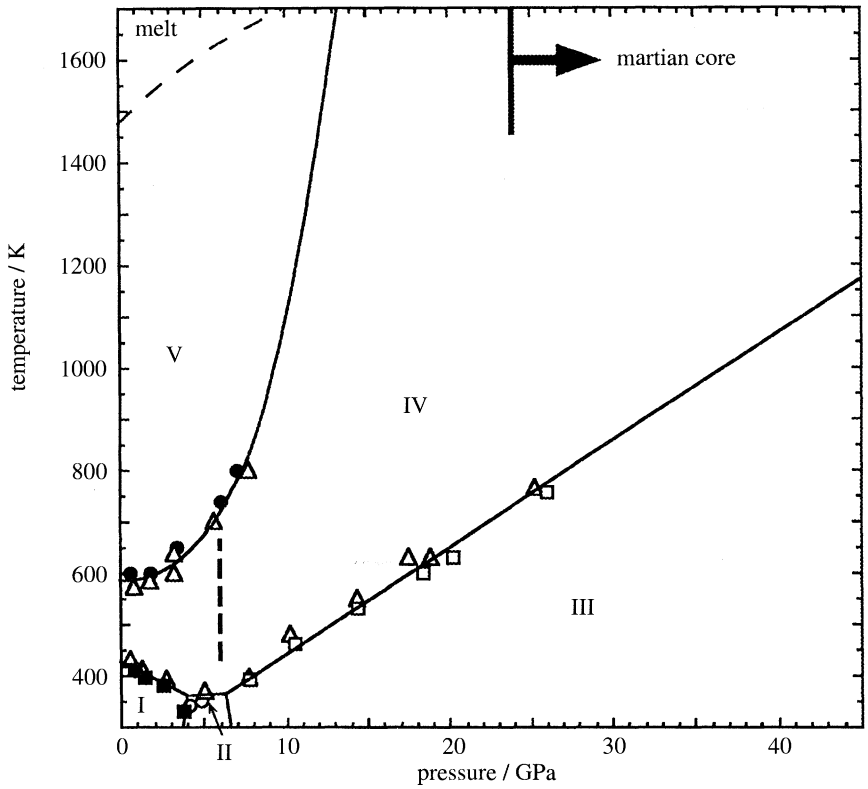

Figure 4. P–T phase diagram of FeS (Fei *et al.* 1995). The boundaries among phases I–IV are determined by X-ray diffraction with resistance-heated diamond cells. Phase IV, which has NiAs (B8) structure, is pertinent to the P–T conditions of the Martian core as indicated.

remain cool and undisturbed. The large temperature gradient and the small heating spot are essential for achieving these extreme P–T conditions, but they also contribute to the uncertainty in defining the precise P–T conditions. Definitive study requires measurement of basic physical properties (identifications of high P–T phase and P–V–T determination) *in situ* on well-defined P–T points within the heated spot. Most laser-heated samples have been studied after temperature quench, while in others, indirect measurements, such as determination of power–temperature relations or textural observations of melting, have been used. Consequently, laser-heated diamond-cell experiments have often been perceived as disequilibrium and ambiguous.

The putative ambiguity is not an intrinsic problem of laser heating. Rather, it reflects the lack of precise *in situ* measurements of sample properties as a function of the temperature distribution. The situation is analogous to the early-on proposed uncertainty in high pressures generated on a small area (10–100 μm) in a diamond cell by building a steep pressure gradient in the sample gasket. Only two decades ago (Mao & Bell 1976), most measurement techniques did not have sufficient resolution for resolving the pressure in such a sample area, thus the pressures were perceived as ambiguous. With the development of microsampling techniques, the sample size no longer presents a problem for defining pressures. Similarly, the laser-heating technique has advanced to new levels of sophistication as a result of the recent technical advances. The problem is not the absolute temperature gradient, but the spatial and

Downloaded from rsta.royalsocietypublishing.org

temporal resolution of the sampling techniques relative to the temperature gradient and stability. It is reassuring that concerted advances have been made in several areas, including developments of microprobing techniques, stabilization for both mid-IR (CO_2) and near-IR (Nd:YAG or YLF) lasers (see Syono & Manghnani 1992), and improvements in optics.

Significant progress has also been made in shaping and defining the radial and axial temperature gradients. The radial temperature gradient can be accurately determined by mapping the grey-body thermal emission spectra with optical microprobes consisting of imaging spectrographs and area (CCD) detectors. The typically used TEM_{00} laser mode has a Gaussian-like power distribution, producing a bell-shaped peak in the hot spot (Heinz 1990). Although the FWHM of a focused hot spot of a YAG laser is approximately 30 μm in diameter, the spot within 10% of the maximum temperature is only 5 μm. On the other hand, a multimode laser has a flat-top power distribution with five times higher total power than TEM_{00}. In addition, an optical fibre and aperture can be used to produce an intermediate image spot with a flat power distribution and a sharp edge. The spot is refocused through the 30° conical aperture of the diamond cell to a hot spot with a boxcar-shaped power distribution (full-width-90%-maximum of 50 μm).

The problem of axial gradient (along the direction of the laser beam) can be resolved by heating and measuring from both sides of the sample. Preliminary results are shown in figure 5 (Shen *et al.* 1996). The sample consisted of a platinum foil (20 μm thick) which was sandwiched between MgO media and compressed in a diamond cell to 11 GPa. A multimode YAG laser beam was up-collimated and split into two beams through opposing diamond windows to heat the platinum–MgO interfaces from both sides (A- and B-sides in figure 5) simultaneously. The splitting ratio was adjusted by the feedback of temperature measurements to eliminate the difference of the two sides, so that the axial temperature gradient with the Pt sample vanished. The radial temperature profiles were measured at 3 μm steps. Uniform temperature of 2050 ± 10 K was achieved in a 20 μm diameter × 20 μm thick cylindrical volume of the platinum sample at high pressures (figure 5).

Meanwhile, the spatial resolution of X-ray diffraction microprobe has reached 3 μm (Mao & Hemley 1996), and that of Raman and infrared microprobes have reached the diffraction limit (e.g. 1–10 μm) of the probing radiation, all considerably smaller than the laser-heated hot spot. The microprobes can be used for *in situ* identifications of solid and melt phases within a hot spot. With these developments, the goal of attaining the precision and accuracy of conventional multicomponent phase equilibria with the laser-heated diamond cell is within reach.

6. X-ray diffraction

X-ray diffraction at high pressures provides information on two of the most fundamental properties: crystal structure and P–V equation of state. Under ideal conditions, the accuracy of polycrystalline X-ray diffraction can reach $\Delta d/d = 0.1\%$ for energy dispersive and 0.02% for angular dispersive experiments. At ultrahigh pressures, however, the ideal conditions are seldom met: deviatoric stresses and grain-size effect degrade accuracy, introducing systematic errors of up to $\Delta d/d = 0.5\%$. Deviatoric stresses can be reduced by the use of quasi-hydrostatic pressure media, or directly measured by probing the strains as a function of the angle to the load axis or from the dependence of measured lattice parameters on orientation (hkl). Grain-size

Downloaded from rsta.royalsocietypublishing.org

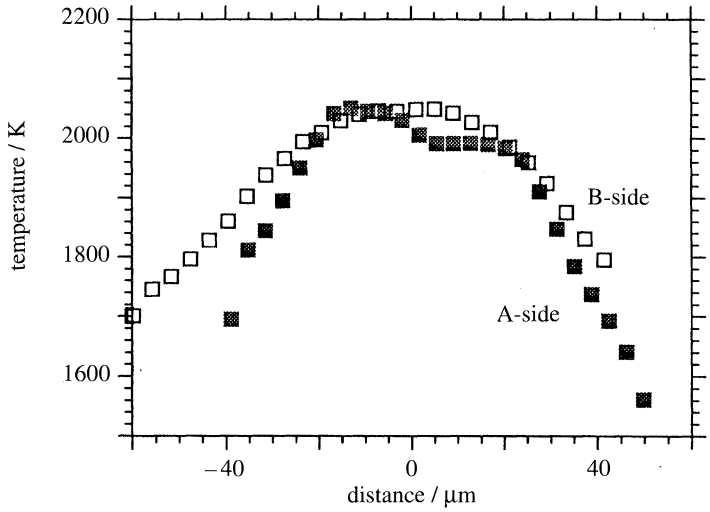

Figure 5. Temperature profiles of a platinum foil heated simultaneously by a YAG laser from two sides. The 50 K temperature step near the centre of the A-side results from change in thickness of the MgO insulating layer, and is not an intrinsic problem.

effects become more pronounced with small X-ray beams that sample an insufficient number of crystallites for satisfying the statistics of a randomly oriented polycrystalline sample.

When the microprobe beam size approaches the dimension of an individual crystal, however, this drawback can be converted into an advantage: a crystallite in the multiple crystal sample may be examined by the techniques of single-crystal X-ray diffraction. Single-crystal diffraction yields considerably more information and is more accurate than polycrystalline diffraction. Uncertainties in peak positions and intensities caused by overlapping reflections in a polycrystalline pattern do not present a problem for single-crystal diffraction because two reflections are well separated in reciprocal space. For each diffraction condition satisfied for each single crystal, only one peak (*hkl*) and its overtones (*nh nk nl*) are present. In a helium pressure medium, the range for meeting the condition is very small (rocking curve range less than 0.1°), so reflections can be resolved despite twining, multiple crystals and mosaic spreading. Moreover, the peaks related by symmetry (same class) occur at different orientations (reciprocal space), which therefore permits the detection of minute changes in symmetry caused by displacive phase transition or deviatoric stresses.

Again, there are trade-offs. Since X-ray reflections occur in specific orientations, access to a large region of reciprocal space (usually a 90° cone) is needed to cover a sufficient number of reflections for analysis. The 90° opening automatically limits the diamond-cell length/diameter ratio to less than 1, thereby sacrificing the stability of the long piston-cylinder configuration. Figure 6*a* shows a new design of a short piston-cylinder cell modified from the Merrill–Bassett cell and GL single-crystal cell (Mao 1989) to optimize the stability with the 90° opening. The cell has been used to study a single-crystal stishovite to 65 GPa (Mao *et al.* 1994). The stishovite crystal was immersed in hydrogen as a hydrostatic pressure medium in a 70 μm diameter sample chamber. We observed a reversible phase transition from stishovite to $CaCl_2$ structure at 56 GPa on increasing pressure and 40 GPa on releasing pressure. The observations of splitting of *hkl* diffraction (figure 7) and non-splitting of *hhl* diffraction indicate

Downloaded from rsta.royalsocietypublishing.org

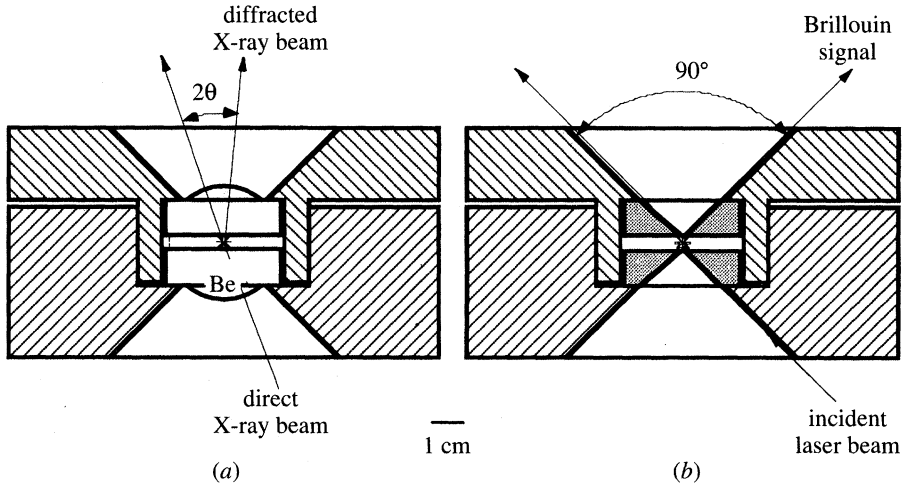

Figure 6. Diamond cells with large access angle (90° cone): (*a*) for single-crystal X-ray diffraction and (*b*) for Brillouin scattering measurements.

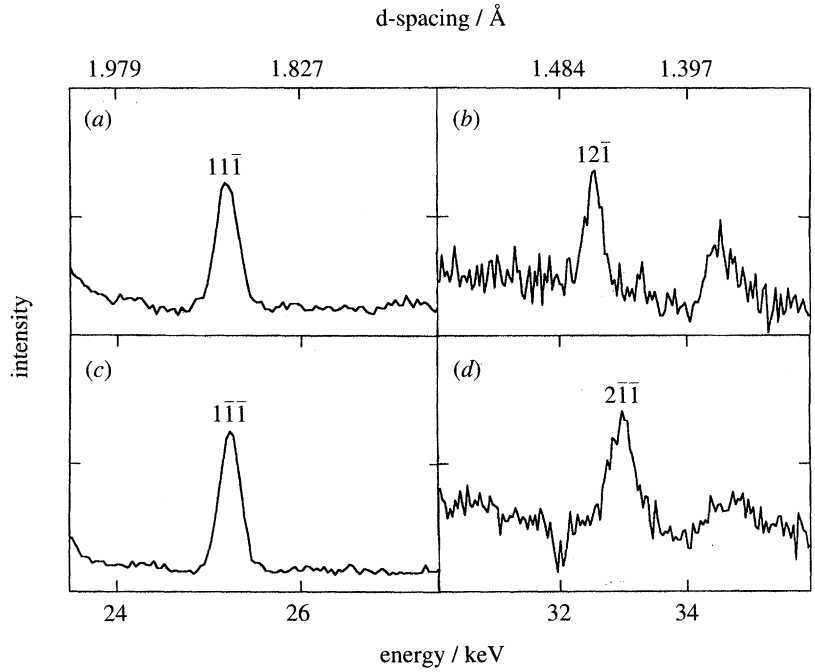

Figure 7. Single-crystal energy dispersive X-ray diffraction pattern of stishovite at 65.37 GPa, $2\theta = 15°$, $Ed = 47.495$ keV Å. Orientations indicated by values of χ and ω: (*a*) $\omega = 1.5°$, $\chi = 37.2°$; (*b*) $\omega = -1.095°$, $\chi = 18.2°$; (*c*) $\omega = 10.345°$, $\chi = 92.716°$; (*d*) $\omega = 27.495°$, $\chi = 85.0°$. The *d*-spacings of $1\,2\,\bar{1}$ and $2\,\bar{1}\,\bar{1}$ reflections are different while those of $1\,1\,\bar{1}$ and $1\,\bar{1}\,\bar{1}$ reflections remain degenerated, indicating a transition from tetragonal to orthorhombic unit cell.

the transition is a distortion of the tetragonal stishovite to the orthorhombic $CaCl_2$ structure.

The maximum applicable force of the single-crystal cell is limited by the strength of the beryllium seat. Within the force constraint, higher pressures (greater than

Downloaded from rsta.royalsocietypublishing.org

65 GPa) require reduction of the sample chamber size (less than 70 μm). An alternative trade-off is to reduce the 90° opening and to replace the Be seat with a harder material that is still transparent to X-rays. Recently, single-crystal X-ray diffraction of hydrogen has been studied successfully up to 120 GPa with a diamond cell with boron seats and a 70° opening (Loubeyre *et al.* 1996).

7. Brillouin scattering

Brillouin spectroscopy provides information on acoustic velocities which are directly comparable to seismic data, the primary source of information on structure and state of the Earth's deep interior (Bassett & Brody 1977; Yeganeh-Haeri *et al.* 1989). The pressure dependence of second-order single-crystal elastic moduli can be determined; from this the aggregate shear and bulk moduli can be obtained. Despite their key importance, high-pressure or high-temperature elasticity data are scarce (Webb 1989; Yoneda & Morioka 1992; Zaug *et al.* 1993) and simultaneous high P–T results are essentially non-existent for lower mantle conditions. High-pressure Brillouin spectroscopy has been a promising technique for mineral physics in the past decade, but its potential has not been realized because of experimental difficulties: (*a*) for the most meaningful measurements, the sample must remain as a clean unstressed single crystal; (*b*) measurements over a wide range of orientation are needed to constrain a number of elastic moduli (three in a cubic crystal, up to 27 in a triclinic crystal); (*c*) the Brillouin signal is very weak in comparison to that of the excitation laser background. Recent advances have alleviated or resolved these problems. Single crystals of a wide variety of materials (oxides, silicates and even hydrogen) can be preserved to 100 GPa in helium pressure media in diamond cells. Conical access of 90° allows Brillouin measurements in all 360° directions around the diamond cell axis (figure 6*b*).

With a very stable optical system and diamond cell, the weak Brillouin signal can be accumulated over long time (e.g. 24 hours) to enhance the S/N ratio. Acoustic velocities in different directions of a small (10–20 μm thickness) single crystal can be measured at high pressures. Elasticity of single-crystal hydrogen has been determined to 24 GPa (Zha *et al.* 1993); the results have been applied for interpreting seismic models of Jupiter (Duffy *et al.* al 1994). Nine elastic moduli of a single-crystal forsterite have been determined as a function of pressure to 16 GPa (Zha *et al.* 1994*a*, *b*). Results are plotted in figure 8 and compared with data of ultrasonic (Graham & Barsch 1969; Kumazawa & Anderson 1969; Webb 1989; Yoneda & Morioka 1992) and impulsive stimulated scattering (ISS) (Zaug *et al.* 1993) measurements. High-pressure Brillouin measurements have also been performed on single-crystal β-$MgSiO_4$ (figure 9). Because the mantle seismic discontinuity at 410 km (14 GPa) is caused by the α–β transition of olivine, the results constrain the composition of the mantle to less than 40% olivine (Duffy *et al.* 1995).

For Brillouin measurements at pressures higher than 50 GPa and at high temperatures, we face a trade-off. The seat with 90° opening will be too weak to support diamonds at large force. The cell in figure 2*b* provides sufficient support for resistive heating to the maximum temperature, but the access is limited. The small opening only allows access of one orientation; multiple prealigned single crystals are necessary for measurements of multiple orientations. For isotropic materials, however, one orientation is sufficient, as shown in the Brillouin study of acoustic velocity and refractive index of SiO_2 glass up to 60 GPa (Zha *et al.* 1994*a*, *b*).

PHILOSOPHICAL TRANSACTIONS OF THE ROYAL SOCIETY A MATHEMATICAL, PHYSICAL & ENGINEERING SCIENCES
PHILOSOPHICAL TRANSACTIONS OF THE ROYAL SOCIETY A MATHEMATICAL, PHYSICAL & ENGINEERING SCIENCES

Downloaded from rsta.royalsocietypublishing.org

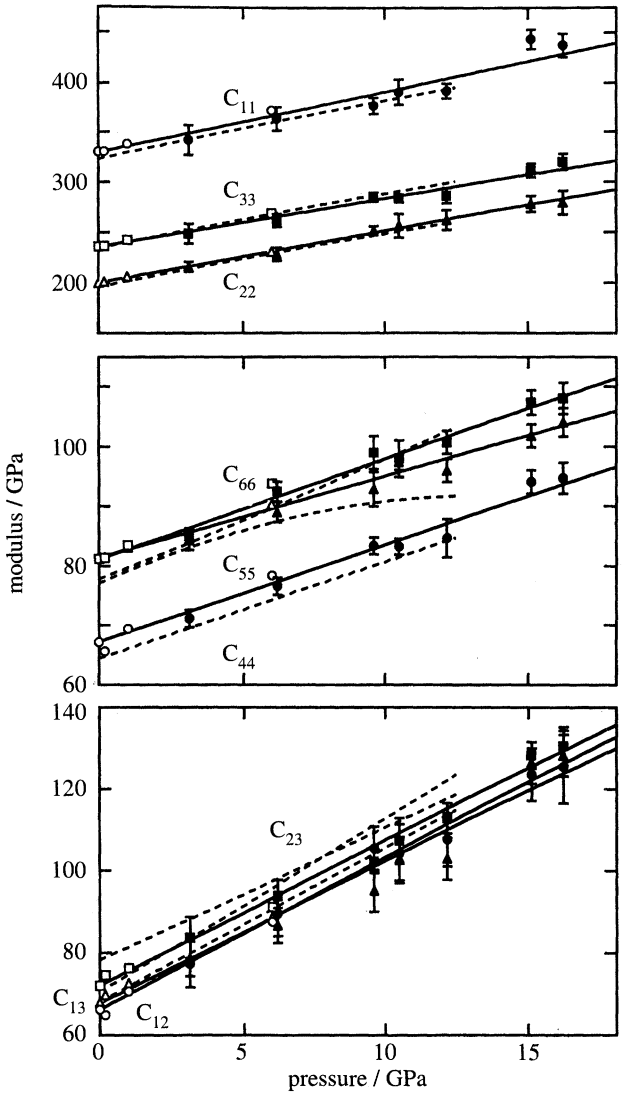

Figure 8. Single-crystal elastic moduli determined by Brillouin-scattering spectroscopy (solid circle and curve) as a function of pressure (Duffy *et al.* 1995). Ultrasonic data (open symbols, Graham & Barsch 1969; Kumazawa & Anderson 1969; Webb 1989; Yoneda & Morioka 1992) and ISS data (dashed curve, Zaug *et al.* 1993) are plotted for comparison.

8. Pressure calibration

In all high-pressure studies, accuracy of pressure determination is, of course, of central importance. Pressure calibration based on the ruby fluorescence scale has been widely used (Forman *et al.* 1972; Mao *et al.* 1978). However, the calibration, including its later extension (Bell *et al.* 1986) and modification for quasi-hydrostatic conditions (Mao *et al.* 1986), was based on technology of the previous decade. Now high-precision measurements can resolve 0.01 GPa at 10 GPa, but pressure accuracy has not improved because the primary calibration based on shock-wave data still carries a 5% uncertainty. Calibration at high temperatures based on equations of state of gold or NaCl is even poorer.

Downloaded from rsta.royalsocietypublishing.org

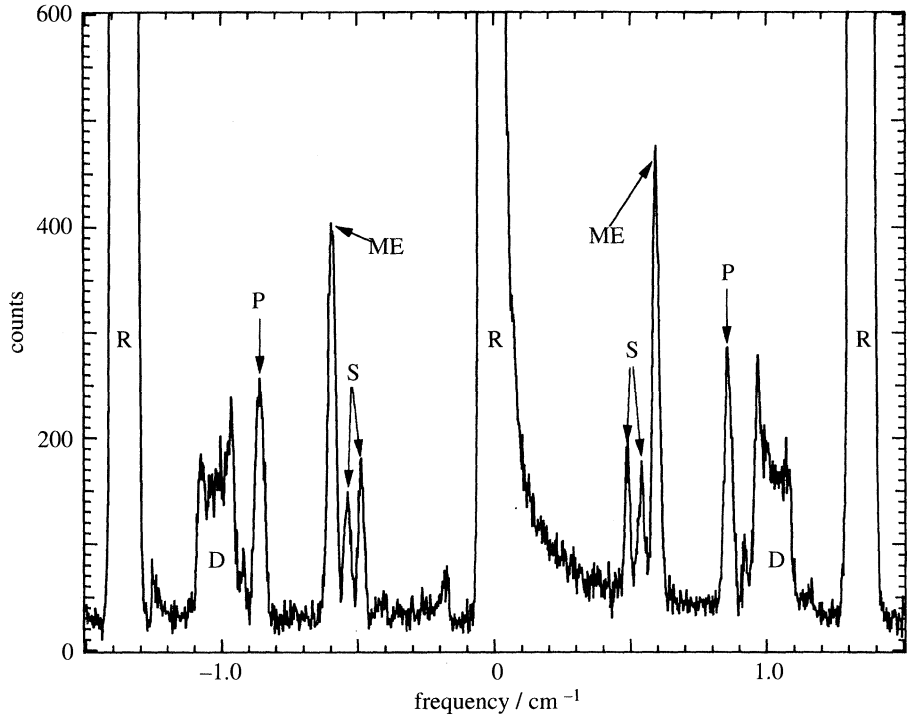

Figure 9. Brillouin-scattering spectrum of a single-crystal β-$MgSiO_4$ at 10.5 GPa. The angle between the incident and scattered beams is 100°. A compressional (P) and two shear waves (S) of β-$MgSiO_4$ are observed. Other peaks are due to Brillouin scattering of diamond anvils (D) and methanol–ethanol pressure medium (ME) and Raleigh scattering of the excitation laser (R).

Ideally, future high P–T pressure scales should be based only on high-precision measurements under hydrostatic conditions. This can be achieved by measuring X-ray diffraction and Brillouin scattering on the same sample at the same P–T conditions. Taking an *ab initio* approach without any prior knowledge of the pressure, one can measure the volume (V) from X-ray diffraction and the bulk modulus, ($K = -V(\partial P/\partial V)$), from Brillouin scattering. Numerical integration of the bulk modulus as a function of volume at constant temperature yields an isothermal P–V equation of state. Resistive heating of the sample at various temperatures yields isotherms and forms a complete P–V–T equation of state as a primary pressure standard. There is a minor correction that Brillouin scattering measures adiabatic bulk modulus, $K_S = -V(\partial P/\partial V)_S$, whereas the isothermal bulk modulus, $K_T = -V(\partial P/\partial V)_T$, is required for the isothermal equation of state. They are related by $K_S = K_T(1+\alpha\gamma T)$, where α is the thermal expansion and γ is the Grüneisen parameter. The main term α is provided by the P–V–T equations of state and can be fed back for iterative corrections. This primary calibration should have a pressure accuracy of 1%. Once such a primary scale is established, it can be used to calibrate additional secondary scales, such as Raman shifts of diamond (Aleksandrov *et al.* 1987) and cubic BN, fluorescence shifts of rare-earth-doped YAG (Hess & Schiferl 1992) and equations of state of noble-gas solids, noble metals and alkali halides, as convenient and precise pressure calibrations at variable temperatures.

Diamond is an ideal material for primary calibration to 100 GPa and 1000 K because of its chemical inertness and high symmetry. All experiments in diamond cells

Downloaded from rsta.royalsocietypublishing.org

must be compatible with diamond. Because diamond is cubic, it is sufficient to measure X-ray diffraction and Brillouin scattering for one preoriented diamond plate for determining volume and the elastic moduli. (Note that Brillouin scattering provides velocities of one compressional wave and shear waves in each orientation.) With sufficient spatial resolution, signals from the diamond standard and the anvils can be separated.

9. Conclusion

With the continued development of the megabar diamond-anvil cell and related techniques, P–T conditions throughout the Earth's interior have been reached in the laboratory. Physical and chemical properties and processes can be studied under these conditions with increasing accuracy, precision and sensitivity. Key developments in the areas of resistive heating, laser heating, X-ray diffraction, Brillouin scattering and pressure calibration are essential for continued advances in high-pressure experimentation and should contribute to allied fields of Earth sciences: seismology, geodynamics, geochemistry and planetary geology.

We thank NSF, NASA and CIW for supporting our research.

References

Aleksandrov, I. V., Goncharov, A. F., Zisman, A. N. & Stishov, S. M. 1987 Diamond at high pressures: Raman scattering of light, equation of state, and high-pressure scale. *Soviet Phys. JETP* **66**, 384–390.

Bassett, W. A. & Brody, E. M. 1977 Brillouin scattering: A new way to measure elastic moduli at high pressures. In *High-pressure research—applications in geophysics* (ed. M. Manghnani & S. Akimoto), pp. 519–532. New York: Academic.

Bassett, W. A. & Ming, L. C. 1972 Disproportionation of Fe_2SiO_4 to $2FeO+SiO_2$ at pressure up to 250 kbar and temperatures up to 3000 °C. *Phys. Earth Planet. Int.* **6**, 154–160.

Bassett, W. A., Shen, A. H., Bucknum, M. & Chou, I. M. 1993 A new diamond anvil cell for hydrothermal studies to 10 GPa and −190 °C to 1100 °C. *Rev. Scient. Instrum.* **64**, 2340–2345.

Bell, P. M., Xu, J. & Mao, H. K. 1986 Static compression of gold and copper and calibration of the ruby pressure scale to pressures to 1.8 Mbar. In *Proc. 4th American Physical Society (APS) Topical Conf. on Shock Waves in Condensed Matter* (ed. Y. Gupta), pp. 125–130. New York: Plenum.

Boehler, R. 1992 Melting of the Fe–FeO and the Fe–FeS systems at high pressure: constraints on core temperatures. *Earth Planet. Sci. Lett.* **111**, 217–227.

Boyd, F. R. & England, J. L. 1960 Apparatus for phase-equilibrium measurements at pressures up to 50 kbar and temperatures up to 1750 °C. *J. Geophys. Res.* **65**, 741–748.

Decker, D. L. 1971 High-pressure equation of state for NaCl, KCl, and CsCl. *J. Appl. Phys.* **42**, 3239–3244.

Duffy, T. S., Vos, W. L., Zha, C. S., Hemley, R. J. & Mao, H. K. 1994 Sound velocities in dense hydrogen and the interior of Jupiter. *Science* **263**, 1590–1593.

Duffy, T. S., Zha, C. S., Downs, R. T., Mao, H. K. & Hemley, R. J. 1995 Elasticity of forsterite Mg_2SiO_4 to 16 GPa and the composition of the upper mantle. *Nature* **378**, 170–173.

Fei, Y. & Mao, H. K. 1994 *In situ* determination of the NiAs phase of FeO at high pressure and high temperature. *Science* **266**, 1678–1680.

Fei, Y., Mao, H. K., Shu, J. F., Parthasarathy, G. & Bassett, W. A. 1992 Simultaneous high P–T X-ray diffraction study of β-$(Mg,Fe)_2SiO_4$ to 26 GPa and 900 K. *J. Geophys. Res.* **97**, 4489–4495.

Downloaded from rsta.royalsocietypublishing.org

Fei, Y., Prewitt, C. T., Mao, H. K. & Bertka, C. M. 1995 Structure and density of FeS at high pressure and high temperature and the internal structure of Mars. *Science* **268**, 1892–1894.

Forman, R. A., Piermarini, G. J., Barnett, J. D. & Block, S. 1972 Pressure measurement made by the utilization of ruby sharp-line luminescence. *Science* **176**, 284–285.

Glazkov, V. P., Besedin, S. P., Goncharenko, I. N., Irodova, A. V., Makarenko, I. N., Somenkov, V. A., Stishov, S. M. & Shil'shteyn, S. S. 1988 Investigation of the equation of state of molecular deuterium at high pressure using neutron diffraction. *JETP Lett.* **47**, 661–664.

Graham, E. K. & Barsch, G. R. 1969 Elastic constants of single-crystal forsterite as a function of temperature and pressure. *J. Geophys. Res.* **74**, 5949–5959.

Hanfland, M., Hemley, R. J., Mao, H. K. & Williams, G. P. 1992 Synchrotron infrared spectroscopy at megabar pressures: vibrational dynamics of hydrogen to 180 GPa. *Phys. Rev. Lett.* **69**, 1129–1132.

Heinz, D. L. 1990 Thermal pressure in the laser-heated diamond anvil cell. *Geophys. Res. Lett.* **17**, 1161–1164.

Hemley, R. J., Hanfland, M. & Mao, H. K. 1991 High-pressure dielectric measurements of hydrogen to 170 GPa. *Nature* **350**, 488–491.

Hess, N. J. & Schiferl, D. 1992 Calibration of the pressure-induced frequency shift of Sm:YAG using the ruby and nitrogen vibron pressure scales from 6–900 K and 0–300 kbar. *J. Appl. Phys.* **71**, 2082–2085.

Ishizuka, M. & Amaya, K. 1994 Magnetic measurements under ultrahigh pressure. *IEEE Trans. Magnet.* **30**, 1048–1051.

Ito, E. & Takahashi, E. 1989 Post-spinel transformations in the system Mg_2SiO_4–Fe_2SiO_4 and some geophysical implications. *J. Geophys. Res.* **94**, 10 637–10 646.

Jeanloz, R. & Ahrens, T. J. 1980 Equations of state of FeO and CaO. *Geophys. Jl R. Astr. Soc.* **62**, 505–528.

Knittle, E. & Jeanloz, R. 1991 The high-pressure phase diagram of $Fe_{0.94}O$: a possible constituent of the Earth's core. *J. Geophys. Res.* **96**, 16 169–16 180.

Kumazawa, M. & Anderson, O. L. 1969 Elastic moduli, pressure derivatives, and temperature derivatives of single-crystal olivine and single-crystal forsterite. *J. Geophys. Res.* **74**, 5961–5972.

Liu, L. & Bassett, W. A. 1986 *Elements, oxides, silicates.* Oxford University Press.

Loubeyre, P., LeToullec, R., Hausermann, D., Hanfland, M., Hemley, R. J., Mao, H. K. & Finger, L. W. 1996 Single-crystal X-ray diffraction of hydrogen up to 120 GPa. *Nature* (Submitted.)

Luth, W. C. & Tuttle, O. F. 1963 Externally heated cold-seal pressure vessels for use to 10 000 bars and 750 °C. *Am. Mineral.* **48**, 1401–1403.

Manghnani, M. H. & Syono, Y. (eds) 1987 *High pressure research in mineral physics.* Geophys. Monograph 39, Mineral Phys., vol. 2, pp. 486. Tokyo: Terra.

Mao, H. K. 1989 Static compression of simple molecular systems in the megabar range. In *Simple molecular systems at very high density* (ed. P. Loubeyre *et al.*), pp. 221–236. New York: Plenum.

Mao, H. K. & Bell, P. M. 1971 High-pressure decomposition of spinel (Fe_2SiO_4). In *Carnegie Institution Washington Yearbook 70*, pp. 176-178.

Mao, H. K. & Bell, P. M. 1976 High-pressure physics: the 1 Mbar mark on the ruby R_1 static pressure scale. *Science* **191**, 851–852.

Mao, H. K., Bell, P. M., Shaner, J. & Steinberg, D. 1978 Specific volume measurements of Cu, Mo, Pd, and Ag and calibration of the ruby R_1 fluorescence pressure gauge from 0.06–1 Mbar. *J. Appl. Phys.* **49**, 3276–3283.

Mao, H. K., Bell, P. M. & Yagi, T. 1979 Iron-magnesium fractionation model for the Earth. *Carnegie Institution Washington Yearbook 78*, 621–625.

Mao, H. K. & Hemley, R. J. 1996 Energy dispersive X-ray diffraction of micro-crystals at ultrahigh pressures. *High Pressure Res.* (In the press.)

Mao, H. K., Hemley, R. J., Fei, Y., Shu, J. F., Chen, L. C., Jephcoat, A. P., Wu, Y. & Bassett, W. A. 1991 Effect of pressure, temperature, and composition on lattice parameters and density of (Fe,Mg)SiO_3-perovskites to 30 GPa. *J. Geophys. Res.* **96**, 8069–8079.

PHILOSOPHICAL TRANSACTIONS OF THE ROYAL SOCIETY A MATHEMATICAL, PHYSICAL & ENGINEERING SCIENCES

PHILOSOPHICAL TRANSACTIONS OF THE ROYAL SOCIETY A MATHEMATICAL, PHYSICAL & ENGINEERING SCIENCES

Downloaded from rsta.royalsocietypublishing.org

Mao, H. K., Hemley, R. J. & Mao, A. L. 1994 Recent design of ultrahigh-pressure diamond cell. In *High pressure science and technology—1993* (ed. S. C. Schmidt, J. W. Shaner, G. A. Samara & M. Ross), vol. 2, pp. 1613–1616. New York: AIP.

Mao, H. K., Shu, J., Hu, J. & Hemley, R. J. 1994 Single-crystal X-ray diffraction of stishovite to 65 GPa. *Eos* **75**, 662.

Mao, H. K., Wu, Y., Chen, L. C., Shu, J. F. & Jephcoat, A. P. 1990 Static compression of iron to 300 GPa and $Fe_{0.8}Ni_{0.2}$ alloy to 260 GPa: implications for composition of the core. *J. Geophys. Res.* **95**, 21 737–21 742.

Mao, H. K., Xu, J. & Bell, P. M. 1986 Calibration of the ruby pressure gauge to 800 kbar under quasihydrostatic conditions. *J. Geophys. Res.* **91**, 4673–4676.

Meade, C., Hemley, R. J. & Mao, H. K. 1992 High pressure X-ray diffraction of SiO_2 glass. *Phys. Rev. Lett.* **69**, 1387–1390.

Ming, L. C., Manghnani, M. H., Balogh, J., Qadri, S. B., Skelton, E. F. & Jamieson, J. C. 1983 Gold as a reliable internal pressure calibrant at high temperatures. *J. Appl. Phys.* **54**, 4390–4397.

Poirier, J.-P. 1991 *Introduction to the physics of the Earth interior*, pp. 264. Cambridge University Press.

Saxena, S. K., Dubrovinsky, L. S., Haggkvist, P., Cerenius, Y., Shen, G. & Mao, H. K. 1995 Synchrotron X-ray study of iron at high pressure and temperature. *Science* **269**, 1703–1704.

Shen, G., Mao, H. K. & Hemley, R. J. 1996 In *Laser-heating diamond-cell technique: double-sided heating with multimode ND:YAG laser* (ISAM96, Tsukuba, Japan). (In the press.)

Stixrude, L., Hemley, R. J., Fei, Y. & Mao, H. K. 1992 Thermoelasticity of silicate perovskite and magnesiowüstite and stratification of the Earth's mantle. *Science* **257**, 1099–1101.

Syono, Y. & Manghnani, M. H. (eds) 1992 *High pressure research in mineral physics: application to earth and planetary sciences*, Geophys. Monograph 67, Mineral Phys., vol. 3, pp. 530. Tokyo: Terra.

Vos, W. L., Finger, L. W., Hemley, R. J., Hu, J.-Z., Mao, H. K. & Schouten, J. A. 1992 A high-pressure van der Waals compound in solid nitrogen–helium mixtures. *Nature* **358**, 46–48.

Vos, W. L., Finger, L. W., Hemley, R. J. & Mao, H. K. 1993 Novel H_2–H_2O clathrate at high pressures. *Phys. Rev. Lett.* **71**, 3150–3153.

Webb, S. L. 1989 The elasticity of the upper mantle orthosilicates olivine and garnet to 3 GPa. *Phys. Chem. Mineral.* **16**, 684–692.

Xu, J., Mao, H. K. & Bell, P. M. 1986 High pressure ruby and diamond fluorescence: Observations at 0.21 to 0.55 TPa. *Science* **232**, 1404–1406.

Yagi, T., Bell, P. M. & Mao, H. K. 1979 Phase relations in the system magnesium oxide–iron (II) oxide–silicon dioxide between 150 and 700 kbar at 1000 °C. *Carnegie Institution Washington Yearbook 78*, pp. 614–616.

Yeganeh-Haeri, A., Weidner, D. J. & Ito, E. 1989 Elasticity of $MgSiO_3$ in the perovskite structure. *Science* **243**, 787–789.

Yoneda, A. & Morioka, M. 1992 Pressure derivatives of elastic constants of single crystal forsterite. In *High-pressure research: application to earth and planetary sciences* (ed. Y. Syono and M. H. Manghnani), pp. 207–214. Tokyo: Terra.

Yoo, C. S., Akella, J., Campbell, A., Mao, H. K. & Hemley, R. J. 1995 Phase diagram of iron by in-situ X-ray diffraction: implications for the Earth's core. *Science* **270**, 1473–1475.

Zaug, J., Abramson, E., Brown, J. M. & Slutsky, L. J. 1992 Elastic constants, equations of state and thernal diffusivity at high pressure. In *High pressure research: application to Earth and planetary sciences*, Geophys. Monograph 67, Mineral Phys. (ed. Y. Syono and M. H. Manghnani), vol. 3, pp. 157–166. Tokyo: Terra.

Zaug, J. M., Abramson, E. H., Brown, J. M. & Slutsky, L. J. 1993 Sound velocities in olivine at Earth mantle pressures. *Science* **260**, 1487–1489.

Zha, C. S., Duffy, T. S., Mao, H. K. & Hemley, R. J. 1993 Elasticity of hydrogen to 24 GPa from single-crystal Brillouin scattering and synchrotron X-ray diffraction. *Phys. Rev.* B **48**, 9246–9255.

Zha, C. S., Duffy, T. S., Downs, R. T., Mao, H. K. & Hemley, R. J. 1994*a* Single-crystal elasticity of forsterite to 16 GPa. *Eos* **75**, 633.

PHILOSOPHICAL TRANSACTIONS OF THE ROYAL SOCIETY A MATHEMATICAL, PHYSICAL & ENGINEERING SCIENCES

PHILOSOPHICAL TRANSACTIONS OF THE ROYAL SOCIETY A MATHEMATICAL, PHYSICAL & ENGINEERING SCIENCES

Downloaded from rsta.royalsocietypublishing.org

Zha, C. S., Hemley, R. J., Mao, H. K., Duffy, T. S. & Meade, C. 1994*b* Acoustic velocities and refractive index of SiO_2 glass to 57.5 GPa by Brillouin scattering. *Phys. Rev.* B **50**, 13 105–13 112.

Zharkov, V. N. & Gudkova, T. V. 1992 Modern models of giant planets. In *High pressure research in mineral physics: application to Earth and planetary sciences*, Geophys. Monograph 67, Mineral Phys. (ed. Y. Syono & M. H. Manghnani), vol. 3, pp. 393–401. Tokyo: Terra.

PHILOSOPHICAL TRANSACTIONS OF THE ROYAL SOCIETY A MATHEMATICAL, PHYSICAL & ENGINEERING SCIENCES

PHILOSOPHICAL TRANSACTIONS OF THE ROYAL SOCIETY A MATHEMATICAL, PHYSICAL & ENGINEERING SCIENCES